Response to referee #1

We would like to sincerely thank the reviewer for the careful and constructive evaluation of our manuscript. Before addressing the specific comments, we note that the ASI site has been excluded from the revised manuscript due to unresolved instrumental issues as detailed in Che et al. (2025) and in our response to major comment 6 from referee #3. Following the removal of ASI, the text, analyses, tables, and figures have been revised accordingly to ensure internal consistency. In addition, following a suggestion from referee #3, the Appendix has been removed. All material previously included in the Appendix has been moved to the Supplement under the section *"Shen methodology"*, and a new section describing the *Random Forest model performance* has been added.

A point-by-point response to all comments is provided below. Our responses are presented in bold, while the corresponding modifications introduced in the revised manuscript are shown here *in italics and within quotation marks*. Text that has been removed from the manuscript is crossed out where relevant and all changes implemented in the revised version of the manuscript are highlighted in red.

This manuscript evaluates several different cloud condensation nuclei (CCN) prediction methods, including a couple of new ones derived here, against long-term measurements conducted at 10 different continental sites. The topic of the conducted research is a very important one. Both the technical approach and scientific conclusions made from the data appear robust. Overall, the paper is very well written and properly organized. I recommend accepting the paper for publication after a few, relatively minor revisions.

1) It is mentioned that the 3 mountain sites considered here have low activated fraction (AF) compared to other high-mountain sites. Does the "other sites" refer to all other sites for which such information is available, or some sub-set of sites in earlier studies? Do the authors have some idea why AF is particularly low at these 3 sites compared with other sites? (lines 327-329).

With the phrase "other high-mountain sites" we referred to values reported in the literature for high-altitude observatories where AF at comparable supersaturations has been reported. In particular, Rejano et al. (2021) reported a mean AF of 0.47 at 0.5% SS during summer at Sierra Nevada (2500 m a.s.l.), Spain. At Jungfraujoch (3580 m a.s.l.) in Switzerland, AF ranged from 0.2 to 0.6 at 0.47% SS throughout the year, with the lowest values (~0.3) observed during winter (Jurányi et al., 2011). Higher AF values (~0.57 at 0.4% SS) were reported at Mt. Lu (1165 m a.s.l.) in East China during Nov-Dec (Duan et al., 2023).

In contrast, our three mountain sites (SBS-CP, GUC, SBS-SPL) exhibit lower median AF at 0.4% SS (0.11, 0.24, and 0.19, respectively). This difference can be partly attributed to a substantial fraction of measurements being collected during winter months, when weaker photochemical aerosol production (Baltensperger et al., 1997; Barbaro et al., 2024) and more persistent free-tropospheric influence (Collaud Coen, 2011; Jurányi et al.,

2011) lead to smaller, less hygroscopic particles and systematically lower AF. Site-specific processes may also contribute: SBS-CP and SBS-SPL are frequently influenced by intercontinental dust (Hallar et al., 2011), and GUC occasionally experiences biomass-burning events (Gibson et al., 2025). These processes can increase total particle concentration while reducing the fraction of particles that activate at moderate supersaturations. We have now clarified these points in the revised manuscript.

Lines 327-329 (lines 334-341 in the revised manuscript)- *'The three mountain sites show low median activated fractions at 0.4% SS (0.11, 0.24, and 0.19 at SBS-CP, GUC, and SBS-SPL, respectively) compared to other high-mountain sites reported in the literature (Jurányi et al., 2011; Rejano et al., 2021; Duan et al., 2023). This difference can be partly attributed to a substantial fraction of measurements being collected during winter months, when weaker photochemical aerosol production (Baltensperger et al., 1997; Barbaro et al., 2024) and more persistent free-tropospheric influence (Collaud Coen, 2011; Jurányi et al., 2011) lead to smaller, less hygroscopic particles and lower AF. Site-specific processes, including intercontinental dust at SBS-CP and SBS-SPL (Hallar et al., 2011) and occasional biomass-burning events at GUC (Gibson et al., 2025), may also contribute to the observed low AF.'*

2) I am not able to follow the logic here. While the bimodalily of Dgeo distribution admittedly suggests a mixture of two sources with very different particle size characteristics influencing the site, how would this bimodality by itself tell anything about the hygroscopicity of particles from these two sources (even when combined with Drit and kappa distributions)? (lines 362-365).

We thank the reviewer for this comment. We agree that the bimodality of the Dgeo distribution alone does not allow direct inference of the hygroscopicity of particles in each mode. The previous statement has been revised to avoid speculation about particle composition based solely on size distribution. We now describe the bimodality as indicative of two dominant particle size modes without attributing specific hygroscopic properties to either mode.

Lines 362-365 (lines 372-374 in the revised manuscript)- '*The bimodal distribution of Dgeo observed at GUC ~~suggests the coexistence of different aerosol types, potentially with distinct hygroscopic properties. The first mode, with values lower than Dcrit, likely corresponds to highly soluble particles such as sulfates. In contrast, the second mode, at larger diameters, may be associated with less hygroscopic aerosols, such as organic compounds related to biomass burning~~ indicates the presence of two distinct aerosol sources influencing the site, such as background continental aerosols and episodic contributions from biomass burning or dust transport, consistent with previous studies (Gibson et al., 2025).'*

3) Associated with the first statement on this line, I would add reference to both Fig. 4a and Table 1, so that the reader can easily confirm the stated fact (line 431).

We have now added explicit references to both Fig. 4a and Table 1 in line 431 (line 435 in the revised manuscript) so that readers can easily verify the comparison between κCCN and κchem across sites. The revised text now reads:

'In general, κCCN is lower than κchem for all sites (see Fig. 4a and Table 1).'

4) The authors correctly point out that different particle size ranges covered by CCNC and ACSM probably influence the comparability between kappaChem and kappaCCN. They should bring up more explicitly the fact that kappaCCN is influenced mainly by the hygroscopicity of particles having sizes close to Drit, while kappaChem is determined by some sort of bulk or "mass-average) hygroscopicity of all particles measured by the ACSM. This implies simply that if particles close to Drit are less (more) hygroscopic than the larger particles making most of sub-micron mass, then kappaCCN is expected to smaller (larger) than kappaChem. The systematically lower kappaCCN at these sites might simply indicate that organic fraction of particles increases with decreasing particle size when approaching Drit. For the same reason outlined above, I think that it is irrelevant to explain differences between kappaChem and kappaCCN by whether Dcrit drops between the lower size cut of ACSM or not (lines 474-479): Dcrit at 0.4% supersaturation is anyhow well below that mass-mean diameter of particles measured by ACSM, so it is not expected that these 2 kappas are the same. There are, of course, many other things (as discussed in literature and to some extend also in section 4 here) that might affect the comparability between kappaChem and kappa CCN, but I feel that this "size-issue" should be mentioned already here (lines 435-439 (and 474-479)).

We have revised the manuscript to more explicitly address the fundamental role of particle size in the comparison between κCCN and κchem. The text now clearly states that κCCN is mainly influenced by the hygroscopicity of particles with dry diameters close to Dcrit, whereas κchem represents a bulk, mass-weighted hygroscopicity dominated by particles measured by the ACSM, with the mass contribution dominated by larger, accumulation-mode particles. We explicitly discuss that κCCN is expected to be lower (higher) than κchem when particles near Dcrit are less (more) hygroscopic than the larger particles dominating submicron mass. Following the reviewer's suggestion, we have removed the emphasis on whether Dcrit falls within the ACSM size range as a primary explanation for the observed differences, and instead treat this effect as secondary and limited to the highest supersaturations at specific sites. These revisions have been implemented in lines 431–439 and 474–479.

Lines 431-439 (lines 435-440 in the revised manuscript) - *'In general, κCCN is lower than κchem for all sites (see Fig. 4a and Table 1). Note that these two parameters cannot be directly compared since κCCN only accounts for activated particles in the CCNC and its calculation depends primarily on the dry aerosol size distribution and CCN concentrations as a function of*

SS, while κchem represents a bulk, mass-weighted hygroscopicity of all particles measured by the ACSM in the 40–1000 nm size range (Watson, 2017). As a result, if particles with diameters close to Dcrit are less (more) hygroscopic than the larger particles dominating submicron mass, κCCN is expected to be smaller (larger) than κchem.

Lines 474-479 (lines 472-478 in the revised manuscript)- *'~~We must consider the effect of the differences in the size ranges of the CCNC and the ACSM. While the CCNC has no lower size cutoff, the ACSM measures particles in the 40–1000 nm size range (Watson et al., 2018), which could lead to an underestimation of the predicted CCN concentrations if Dcrit is smaller than the ACSM lower size cutoff. However, such small Dcrit values are rare: the 10th percentile drops below 40 nm only at ENA (32–33 nm for SS ≥ 0.8%) and at ASI (18–28 nm for SS ≥ 0.4%). Therefore, the ACSM lower size cutoff may cause a slight underestimation of CCN at ASI and, to a lesser extent, at ENA, but provides comparable estimates at the other sites.~~ It must be considered that CCN concentrations predicted from κchem are based on the bulk, mass-weighted hygroscopicity of all particles measured by the ACSM as mentioned in Section 3.2.2. Because the CCNC measures the number of particles activated at the critical supersaturation (Dcrit), and κCCN is inferred from number concentrations, the measured CCN concentration primarily reflects the hygroscopicity of particles near Dcrit. Consequently, if particles around Dcrit are less (or more) hygroscopic than the larger particles dominating the submicron mass, predicted CCN concentration based on κchem may overestimate (or underestimate) the measured CCN concentration'*

5) Finally, the authors could explain, or mention, somewhere why all the calculations presented in the paper correspond to the supersaturation (SS) of 0.4%. This choice is fine, but in the literature also many other values of SS spanning from about 0.1 to 1 % have been reported.

We thank the reviewer for this comment. As indicated in Section 3.1 (lines 299–300) of the manuscript, all calculations are presented at 0.4 % supersaturation because these measurements underwent an additional quality check (see Sect. 2.2), providing higher reliability. While other SS values (0.1-1 %) are commonly reported in the literature, focusing on 0.4 % SS allows a robust comparison across sites. We have updated the manuscript to clarify this choice in the text as follows:

Lines 299-300 (lines 306-309 in the revised manuscript)- *'However, we focus our analysis on 0.4% SS - rather than 0.2% SS used by Schmale et al. (2018) - because the measurements at 0.4% SS underwent an additional quality check (see Sect. 2.2), ensuring greater reliability of the data. While other supersaturations ranging from ~0.1 to 1 % have been reported in the literature, we emphasize 0.4 % SS here to provide the most robust dataset for analysis.'*

References

Baltensperger, U., Gäggeler, H. W., Jost, D. T., Lugauer, M., Schwikowski, M., Weingartner, E., and Seibert, P. (1997). Aerosol climatology at the high-alpine site Jungfraujoch, Switzerland. *Journal of Geophysical Research: Atmospheres, 102*(D16), 19707–19715.

Barbaro, E., Feltracco, M., De Blasi, F., Turetta, C., Radaelli, M., Cairns, W., Cozzi, G., Mazzi, G., Casula, M., Gabrieli, J., Barbante, C., and Gambaro, A. (2024). Chemical characterization of atmospheric aerosols at a high-altitude mountain site: a study of source apportionment. *Atmospheric Chemistry and Physics, 24*, 2821–2835.

Che, H., Zhang, L., Segal-Rozenhaimer, M., Dang, C., Zuidema, P., and Sedlacek, A. J. I. (2025). Aerosol hygroscopicity over the South-East Atlantic Ocean during the biomass burning season – Part 2: Influence of sea salt and burning conditions on CCN hygroscopicity, Atmospheric Chemistry and Physics, 25, 10 987–11 002.

Collaud Coen, M., Weingartner, E., Furger, M., Nyeki, S., Prévôt, A. S. H., Steinbacher, M., and Baltensperger, U. (2011). Aerosol climatology and planetary boundary influence at the Jungfraujoch analyzed by synoptic weather types. *Atmospheric Chemistry and Physics, 11*, 5931–5944.

Duan, J., Chen, Y., Zhang, X., Wang, W., Zhong, S., Li, J., Lu, G., Fang, C., Guo, L., and Fu, P. (2023). Influence of aerosol physicochemical properties on CCN activation during the Asian winter monsoon at the summit of Mt. Lu, China. *Atmospheric Environment, 296*, 119592.

Gannet Hallar, A., Chirokova, G., McCubbin, I., Painter, T. H., Wiedinmyer, C., and Dodson, C. (2011). Atmospheric bioaerosols transported via dust storms in the western United States. *Geophysical Research Letters, 38*, L17802.

Gibson, L. D., Levin, E. J. T., Emerson, E., Good, N., Hodshire, A., McMeeking, G., Patterson, K., Rainwater, B., Ramin, T., and Swanson, B. (2025). Measurement report: An investigation of the spatiotemporal variability in aerosols in the mountainous terrain of the upper Colorado River basin using SAIL-Net. *Atmospheric Chemistry and Physics*, 25, 2745–2762.

Jurányi, Z., Gysel, M., Weingartner, E., Bukowiecki, N., Kammermann, L., and Baltensperger, U. (2011). A 17 month climatology of the cloud condensation nuclei number concentration at the high alpine site Jungfraujoch. *Journal of Geophysical Research: Atmospheres*, 116,975.

Rejano, F., Casans, A., Via, M., Casquero-Vera, J. A., Castillo, S., Lyamani, H., Cazorla, A., Andrews, E., Pérez-Ramírez, D., Alastuey, A., Gómez-Moreno, F. J., Alados-Arboledas, L., Olmo, F. J., and Titos, G. (2021). Activation properties of aerosol particles as cloud condensation nuclei at urban and high-altitude remote sites in southern Europe. *Science of The Total Environment*, 2020.143100.

Response to referee #3 major comments

We thank the referee for the careful evaluation of our manuscript and for the constructive comments provided. Before addressing the specific comments, we would like to explicitly note that data gathered at Ascension Island (ASI) have been excluded from the analysis and consequently from the new version of the manuscript. This decision was made due to unresolved instrumental issues affecting the CCN and SMPS measurements that were not identified during our previous analysis. Importantly, ASI data were not included in the optical-based prediction schemes because of the lack of concurrent optical measurements; therefore, this change has only a minor impact on the overall focus and conclusions of the study. Following the removal of the ASI dataset, the main text, analyses, tables, and figures have been revised accordingly.

Below we address each comment in detail. Our responses are given in bold, while modifications introduced in the revised manuscript are indicated in *italics and within quotation marks*. Text that has been removed from the manuscript is shown as crossed out where relevant. All changes in the revised version are highlighted in red. A point by point response is included below.

This study draws on observational data of aerosol chemical composition, particle size distributions, aerosol optical properties, and cloud condensation nuclei (CCN) number concentrations from ten sites across diverse environments. CCN concentrations are predicted using two approaches: (1) a combination of chemical composition and particle size distributions, and (2) optical properties alone. The results based on optical parameters— derived using both traditional empirical formulas and machine-learning methods—are particularly noteworthy and offer valuable insights. Overall, the manuscript has the potential to be published in Atmospheric Chemistry and Physics (ACP). However, despite the relatively detailed Methods section, several essential methodological and contextual details remain unclear, and the organization of the manuscript would benefit from further refinement. I recommend publication after the authors thoroughly address the following major comments and substantially revise the manuscript.

(1) I believe the primary emphasis of the manuscript should be the section where CCN number concentrations are predicted from aerosol optical properties. The earlier analysis based on chemical composition and particle size distributions using the κ-Köhler theory could be substantially streamlined. The configurations of Scheme 1 and Scheme 2 provide limited additional insight, as the inclusion of black carbon will inevitably reduce overall aerosol hygroscopicity. The authors note that excluding black carbon is common in previous studies, but this likely reflects the absence of black carbon measurements in those datasets; in contrast, many studies that do measure black carbon appropriately include it in their calculations. Scheme 3 is more relevant, as it helps assess potential biases that arise when models apply a uniform hygroscopicity parameter across different environments. Therefore, I recommend focusing only on Scheme 1 and Scheme 3 and providing a shorter, more concise, discussion of this part of the analysis.

We acknowledge the points raised regarding the emphasis on predicting CCN number concentrations from aerosol optical properties and the relative contribution of the κ-Köhler analysis and the different schemes. Despite the primary emphasis of the manuscript being the CCN predictions, we believe that it is important to contextualize the CCN properties based on the aerosol chemical, physical and optical properties, at least in a streamlined way.

Concerning the κ-Köhler predictions schemes, we agree that Scheme 3 offers valuable insights into potential biases when applying a uniform hygroscopicity parameter, and we appreciate reviewer's recommendation to make the discussion of Schemes 1 and 2 more concise. While we recognize that the inclusion of black carbon inevitably reduces overall aerosol hygroscopicity and that many studies incorporate it when measurements are available, our intention was to illustrate the implications of different assumptions in a systematic manner. We believe that presenting all three schemes, even briefly, helps contextualize the variability and uncertainty in CCN predictions across different approaches.

That said, we revised the manuscript (Lines 467-506) to streamline the discussion of Schemes 1 and 2 while maintaining the overall structure that highlights the comparison among the three schemes. Our goal is to synthesize and preserve clarity and completeness without detracting from the emphasis on CCN predictions.

Lines 467-479 (lines 465-478 in the revised manuscript)*- 'Among the three schemes, the coefficient of determination (*R^2*) is virtually identical (0.82-0.83), indicating a similarly strong correlation between predicted and observed CCN concentrations for all schemes. Scheme 1 (Fig. 5a) shows the best overall agreement with observations, with a slope of 1.09 and the lowest median relative bias (13%), indicating a slight overall overprediction. Scheme 2 (Fig. 5b), which is best interpreted as a sensitivity test that indicates the impact of BC rather than as a different predictive approach, shows a slightly higher slope of 1.15 and a median relative bias of 15%, reflecting a slightly higher overprediction compared to observations. Scheme 3 (Fig. 5c), which uses a fixed κchem, exhibits the highest slope (1.22) and the highest median relative bias (24%), pointing to a consistent tendency to overpredict NCCN. It must be considered that CCN concentrations predicted from κchem are based on the bulk, mass-weighted hygroscopicity of all particles measured by the ACSM (40–1000 nm) as mentioned in Section 3.2.2. In contrast, because the CCNC measures the number of particles activated at the critical supersaturation (Dcrit), the measured CCN concentration primarily reflects the hygroscopicity of particles near Dcrit. Consequently, if particles with diameters close to Dcrit are less (or more) hygroscopic than the larger particles dominating the submicron mass, the predicted CCN concentration based on κchem may overestimate (or underestimate) the measured CCN concentration.'*

Lines 480-506 (lines 479-485 in the revised manuscript)*- 'Figure S9 in the Supplement provides further insight into the performance of each scheme across different stations by showing the R2 and median relative bias (MRB) values for each site. Table S7 lists the number*

of data points available per site for each scheme. Continental stations (SGP, COR, GUC) exhibit a good predictive skill with a slight CCN concentration overestimation across schemes, while the marine site (ENA) shows larger sensitivity to hygroscopicity assumptions, largely due to the inability of the ACSM to detect sea-salt aerosol. Despite these limitations, the results are consistent with previous studies (e.g., Schmale et al., 2018), confirming that composition-derived κchem *values improve CCN predictions, while a constant bulk κchem = 0.3 provides a realistic first-order estimate of CCN number concentrations in diverse environments.'*

(2) In the Random Forest prediction section, the authors should report model performance for both the training and test datasets—such as the coefficient of determination—to assess potential overfitting or underfitting. Demonstrating model reliability is necessary before conducting deeper analysis. The authors should also include a table summarizing the key training parameters for each model, such as the number of trees and maximum tree depth. For model validation, I recommend using k-fold cross-validation rather than relying on a single train–test split. Finally, a flowchart illustrating the different models will help readers more clearly understand the input features and output structure of each approach.

We have substantially revised the random forest section to explicitly assess model robustness prior to any interpretative analysis, as recommended by the reviewer. A new section entitled "Random Forest performance" has been added to the Supplement, where all training and test metrics, hyperparameter settings, convergence diagnostics, and supporting figures are presented in detail.

Model performance is now reported for both training and test datasets using the coefficient of determination (R^2), root mean square error (RMSE), and mean absolute error (MAE). Tables R1 and R2 summarize these metrics for the two predicted parameters of the Twomey equation (C and k), considering both predictor configurations: the S2019 AOPs and the expanded All AOPs set. Reporting training and test performance allows direct evaluation of potential overfitting or underfitting.

Overall, results show close agreement between training and test metrics for all cases, indicating that the models capture the available and relevant information, perform consistently across datasets, and exhibit no evidence of under- or overfitting. For parameter *C*, the models show moderate explanatory power (R^2 ~ 0.50 using S2019 AOPs and ~ 0.59 using All AOPs), with comparable RMSE and MAE across training and test datasets. For parameter *k*, predictive skill is lower (R^2 ~ 0.18 and ~ 0.36, respectively), but the similarly consistent performance between training and test datasets indicates stable model behavior. The relatively low variance found for *k* most likely reflects a weak or noisy relationship between the available predictors and *k*, rather than deficiencies in model training or generalization.

S2019 AOPs	**R^2**	**RMSE**	**MAE**
C train	0.50	778 cm^{-3}	478 cm^{-3}
C test	0.48	802 cm^{-3}	480 cm^{-3}
k train	0.18	0.35	0.26
k test	0.18	0.35	0.26

Table R1. Random forest model performance using S2019 AOPs as predictors.

All AOPs	**R^2**	**RMSE**	**MAE**
C train	0.59	709 cm^{-3}	412 cm^{-3}
C test	0.58	720 cm^{-3}	412 cm^{-3}
k train	0.36	0.31	0.22
k test	0.36	0.30	0.22

Table R2. Same as Table 1, but using All AOPs as predictors.

Concerning the RF implementation, it was done using the MATLAB *TreeBagger* algorithm with 500 regression trees. All random forest models were trained using 500 regression trees, with all available predictors sampled at each split, and no explicit constraint on maximum tree depth. Model performance during training was evaluated using out-of-bag (OOB) predictions, which provide an internal cross-validation estimate intrinsic to the algorithm. To verify that the selected number of trees was sufficient, we conducted a convergence analysis of OOB RMSE and R^2 as a function of the number of trees (Figure R1). Both metrics stabilize beyond approximately 400-500 trees for parameters C and k and for both predictor configurations. Based on this analysis, 500 trees were consistently adopted for all models, ensuring stable performance and allowing direct comparability across model configurations.

Regarding model validation, while N-fold cross-validation (we use N to avoid confusion with parameter *k*) is a valid alternative, random forest models inherently provide an internal estimate of generalization error through out-of-bag (OOB) evaluation. Because each tree is trained on a bootstrap sample, predictions for the excluded observations can be used to assess model performance without additional data partitioning (Breiman, 2001). As noted by Hastie et al. (2009), OOB error estimates are almost identical to those obtained using N-fold cross-validation, while allowing model training and validation in a single sequence. The close agreement between OOB estimates and independent test performance observed here supports the robustness of this validation strategy, which is also computationally efficient.

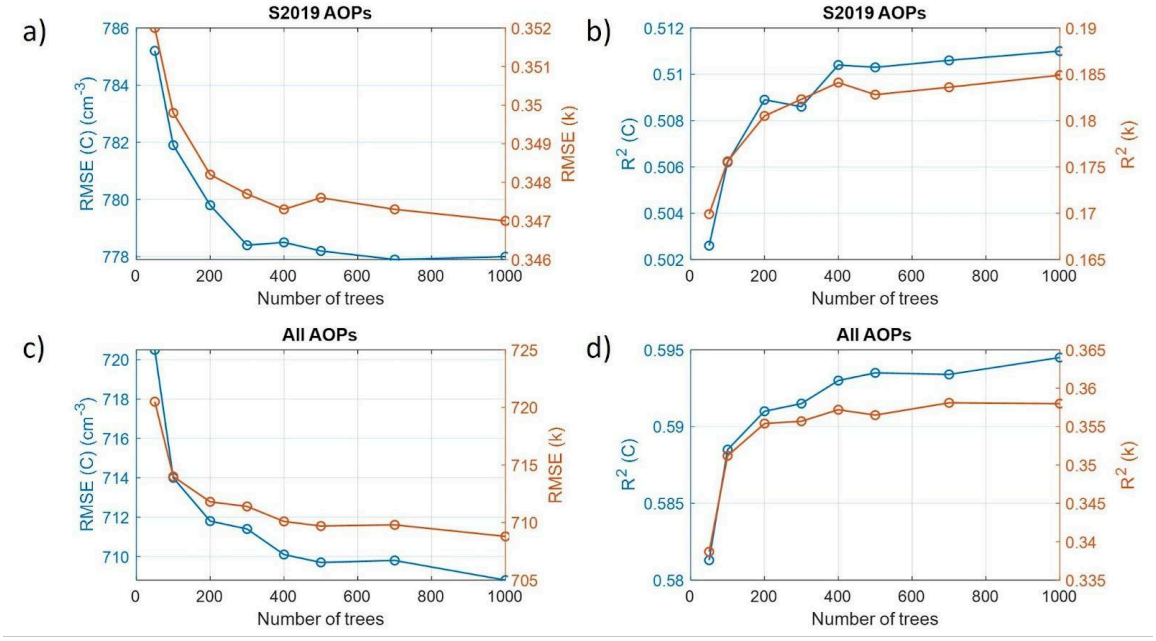

Figure R1: Convergence analysis of random forest model performance as a function of the number of trees for the S2019 AOPs (a–b) and All AOPs (c–d) predictor configurations. Panels (a) and (c) show the evolution of RMSE for C (left axis) and k (right axis), while panels (b) and (d) show the corresponding coefficient of determination (R^2).

Finally, we thank the reviewer for the helpful suggestion of including a flowchart illustrating the different models. It was not entirely clear for us whether the flowchart should illustrate only the random forest models or all CCN prediction methods. We believe that providing an overview of all the CCN prediction approaches can be useful for readers to understand the input features and output structure of each method. Therefore, we have prepared a flowchart summarizing all CCN prediction models and included it in the Supplement (Figure S6 in the new version of the manuscript).

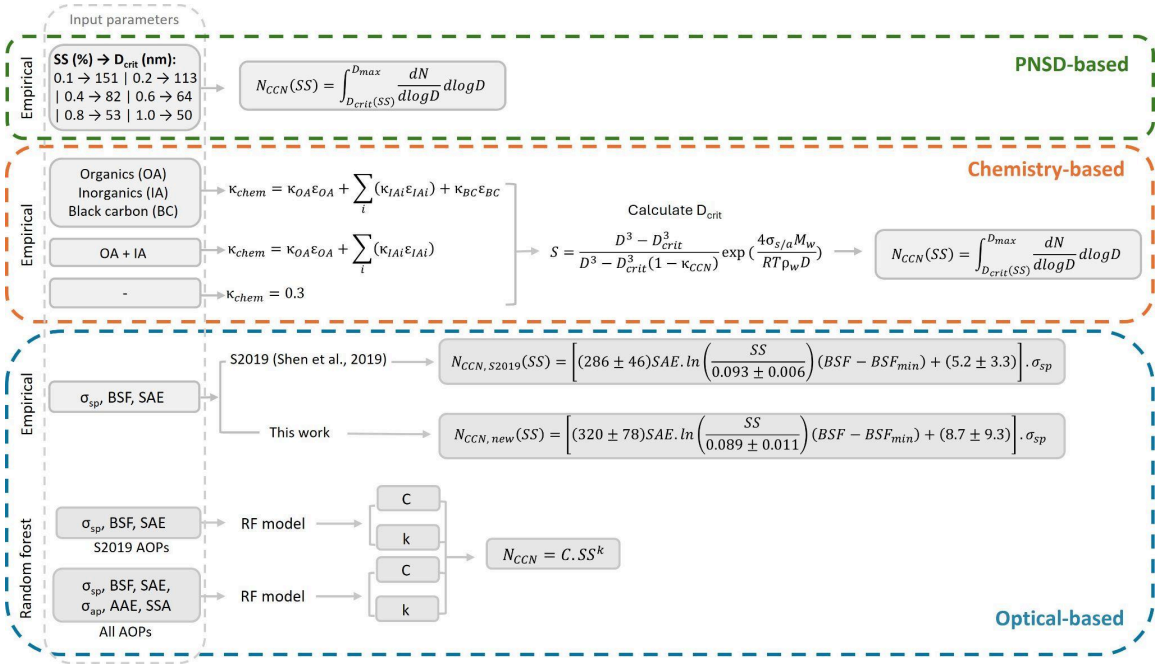

Figure R2: Flowchart of the models used to predict CCN concentrations.

Taking all of the above into account, the changes made to the manuscript are shown below.

Line 205 (line 213 in the revised manuscript)- *'A flowchart summarizing all CCN prediction methods is provided in the Supplement (Figure S6). '*

Line 590-595 (lines 569-576 in the revised manuscript)- *'To further explore the potential of aerosol optical properties to predict CCN concentrations, a random forest model was implemented to estimate the C and k parameters of the Twomey equation. All RF models considered in this work were trained with 500 regression trees, a number selected based on a convergence analysis of out-of-bag RMSE and R^2, which indicated stable model performance for both C and k parameters. Detailed model performance metrics for both training and test datasets including R^2, RMSE, MAE, and hyperparameter settings (number of trees, maximum depth) are provided in the Supplement (Random forest performance section). The close agreement between training and test metrics for both C and k indicates stable model behavior and no evidence of overfitting.'*

Line 614-615 (lines 597-601 in the revised manuscript)- *"Although some of these variables are strongly correlated (see Fig. S13), RF models are known to be robust to multicollinearity (Gregorutti et al., 2017). A full compilation of training and test metrics, as well as RF configuration details for this extended model is provided in the Supplement (Random Forest performance section). The improvement in R^2 and error metrics is consistently observed for both training and test datasets, indicating that the improved performance reflects increased predictive information rather than model overfitting.'*

Line 654-655 (lines 641-643 in the revised manuscript)- *'Therefore, to evaluate the influence of each location on model generalization when considering all AOPs, a LOSO cross-validation approach is applied as explained in section 2.6.3. This analysis is intended to evaluate spatial robustness and site representativeness, rather than to provide an alternative global performance metric to the train–test and OOB evaluations discussed above.'*

(3) The authors base their conclusions of the model performance only on the MSB. However, they should also include a metric regarding the precision, such as RSME. For example, the new equation has a lower bias than the RF models, but e.g. comparing Figs 7b and Fig 9, it might have a larger spread in the predicted vs measured values.

We have revised the discussion section (4. Discussion of CCN prediction methods) to include an additional metric of prediction precision, namely the median absolute error (MdAE), alongside the median relative bias (MRB).

We decided not to include RMSE because it is strongly influenced by a few large deviations, which can disproportionately dominate the metric when combining all supersaturations and sites, potentially leading to misleading comparisons between methods. In contrast, MdAE captures the typical magnitude of deviations in absolute units, providing a more balanced measure of prediction precision.

Accordingly, the discussion has been substantially revised and streamlined to focus more clearly on the comparative performance of the different approaches. Figure 11 has been updated to include panel (b), which shows the MdAE for each prediction method, providing an additional metric of prediction precision. Given that the discussion section has been substantially reorganized and the interpretation of the results has been revised, individual changes are not listed here.

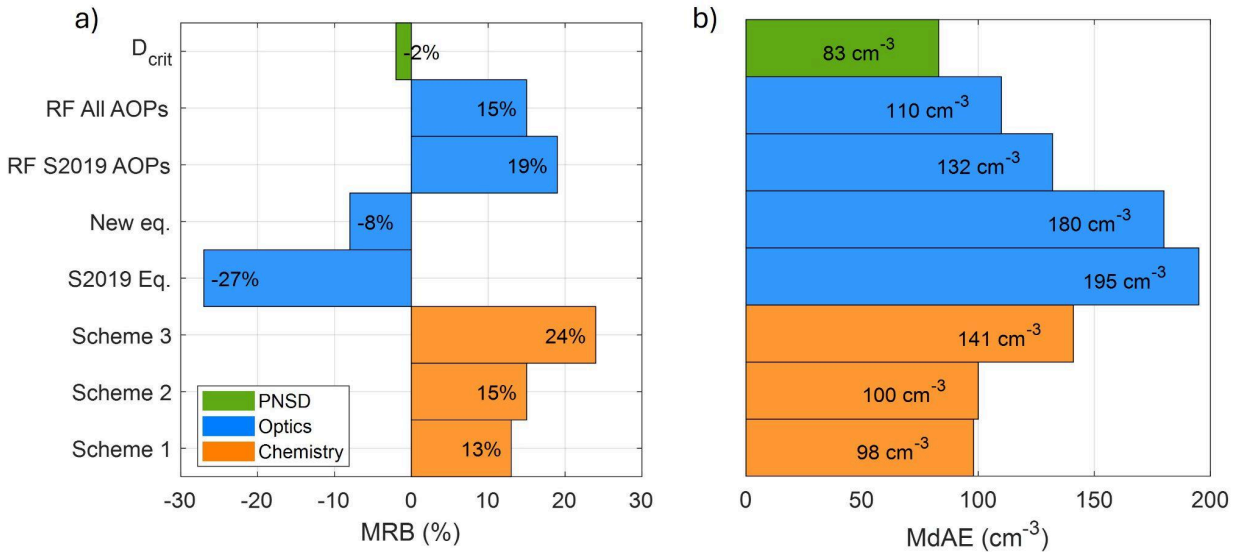

Figure R3. Performance of different CCN prediction methods across all supersaturations and sites. (a) Median relative bias (MRB,%) and (b) median absolute error (MdAE, cm−3) between predicted and measured NCCN. Each box corresponds to a different predictive method applied to the sites with available data.

(4) The authors introduce a new fitting equation for predicting CCN number concentrations from aerosol optical parameters, distinct from the formulation in Shen et al. (2019). This is an important contribution, and the derivation of the new equation should be presented more clearly to improve reader understanding. Currently, the descriptions of both the Shen et al. (2019) equation and the new equation are fragmented, with some content placed in the appendix and additional formulas included below Table S1 in the Supplement. I recommend reorganizing and integrating these materials by presenting the explanation of the Shen et al. (2019) equation alongside the derivation of the new equation in a single, coherent section. This could be either done in the main text or the SI. This restructuring would enhance clarity and help readers follow methodological development more effectively.

We thank the reviewer for the suggestion. To improve readability and facilitate the presentation of the new equation derivation, all content previously in the Appendix has now been moved and reorganized in the Supplement under the section "Shen methodology". In line with the editors' prior recommendation to reduce the overall length of the manuscript, this expanded methodological discussion is presented in the Supplement rather than in the main text. The new section provides a structured and accessible location for the detailed methods, grouping all theoretical steps, figures, and tables in a single, coherent sequence that reflects the correct order of application.

(5) I find that there is some redundancy between the Discussion and Conclusion sections. For example, the description of different methods in previous studies (lines 679–689 in the Discussion) should be more appropriately placed in the Introduction. Similarly, the summary of

the current study's results after line 702 overlaps with content in the Conclusion. I suggest that the authors reorganize and consolidate these sections to make the manuscript more concise and coherent.

We appreciate the reviewer's constructive feedback regarding the redundancy between the Discussion and Conclusion sections. To address this, we have reorganized the manuscript to improve clarity and coherence. As suggested by the reviewer, some references mentioned in the Discussion (lines 679–689) have now been cited in the Introduction to provide context, while avoiding repetition of the detailed methodological descriptions. Additionally, we have modified the Discussion section to include complementary metrics that allow for a more thorough comparison and analysis of the prediction models presented in this study (see major comment #3). In the Conclusions, the description of CCN prediction methods has been condensed, with only a summary provided and no repetition of content already discussed. A summary table (Figure R4; Figure 12 in the new version of the manuscript) has been included to clearly convey the practical recommendations. This table complements the methodological flowchart provided in the Supplement, which presents the description of all methods. These changes ensure that the Discussion provides in-depth analysis, while the Conclusions highlight concise take-home messages, improving the overall clarity and organization of the manuscript.

Category	Method	Input data	Characteristics and recommended use
PNSD-based	D_{crit}	PNSD	Simple and robust; minimal assumptions; reliable CCN estimates when high-resolution PNSD data are available.
Chemistry-based	Scheme 1 (inc. BC)	Bulk chemical comp. + BC + PNSD	Useful when absorption-related effects are relevant; inclusion of BC does not substantially improve CCN prediction.
	Scheme 2 (no BC)	Bulk chemical comp. + PNSD	Captures general CCN activation behavior; when chemical composition data are available but size-resolved chemistry is not.
	Scheme 3 (κ_{chem}=0.3)	PNSD	Simplified first-order CCN estimate; suitable for data-sparse environments, with higher uncertainty.
Optical-based (empirical)	S2019	σ_{sp}, BSF, SAE	Simple empirical approach based on nephelometer measurements.
	New equation	σ_{sp}, BSF, SAE	Bias-reduced empirical approach based on an expanded multi-site dataset; preferred for CCN estimation.
Optical-based (random forest)	RF S2019 AOPs	σ_{sp}, BSF, SAE	Data-driven extension of the Shen-based approach; provides insight into the importance of optical predictors.
	RF All AOPs	σ_{sp}, BSF, SAE, σ_{ap}, AAE, SSA	Data-driven approach; highlights AOPs importance; better performance than RF S2019; suited for exploratory analyses at sites with extensive instrumentation.

Figure R4. Summary of CCN prediction methods evaluated in this study and recommended use.

(6) Page 14, Figure 2/Table 1. The activation diameters at the ASI site seem very low, with the mode of the frequency distribution at 40 nm. For a supersaturation of 0.4%, this corresponds to pure NaCl particles (pure ammonium sulfate particles would have an activation diameter of around 50 nm for S = 0.4%). Since even lower activation diameters down to 30 nm are routinely observed, this seems unlikely and might point to a potential problem with the data. Please do additional quality control and explicitly discuss this issue in the manuscript.

We thank the reviewer for highlighting the unusually low activation diameters observed at the ASI site. Following this comment, we performed extensive additional quality control of both CCN and SMPS measurements at ASI and reviewed existing literature.

Our analysis revealed indications of instrumental issues affecting the ASI measurements. In particular, the recently published paper Che et al. (2025) reported evidence of an instrumental drift or a permanent alteration in the CCN counter from November 2016 onwards, as indicated by shifts in the correlation between CCN concentration at 1% supersaturation ($N_{CCN,1\%}$) and total particle concentration measured by the SMPS ($N_{Tot,\ SMPS}$).

To further investigate, we examined the time series of the ratio between $N_{CCN,1\%}$ and the concentration of particles larger than 30 nm ($N_{>30}$) (Figure R5). This comparison was limited to particles larger than 30 nm to avoid the influence of nucleation-mode particles, which are too small to reliably activate at 1% SS. This ratio should not exceed 1, as the CCN concentration cannot be larger than the number of particles. However, it can be seen that this value starts near 1 in June 2016 and gradually increases over time, consistent with the drift reported by Che et al. (2025). Importantly, such a persistent bias would not necessarily be detected by standard closure metrics based on time-averaged slopes and correlations (Andrews et al., 2025), explaining why the ASI dataset appeared internally consistent in previous analyses but exhibits physically implausible activation diameters when examined in detail here.

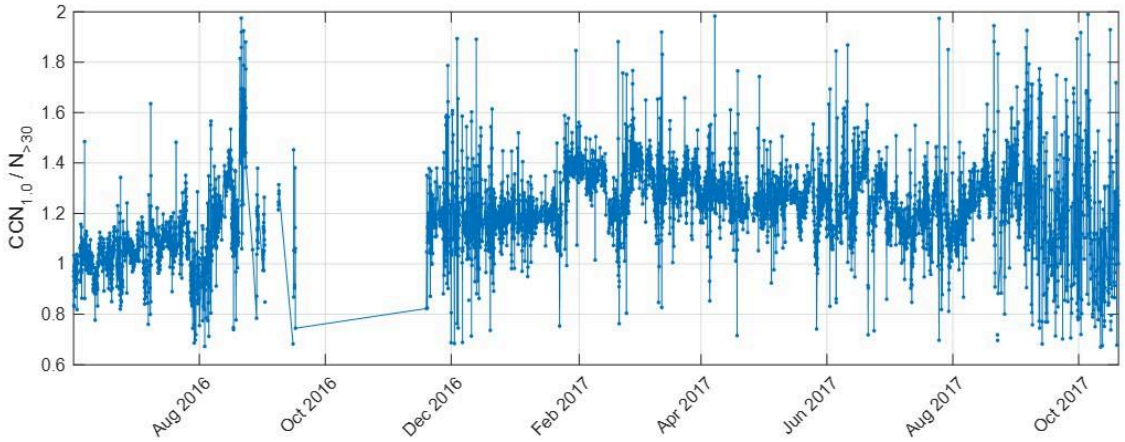

Figure R5: Time series of the ratio between CCN concentration at 1% SS ($N_{CCN,1\%}$) and the concentration of particles larger than 30 nm ($N_{>30}$) at ASI.

Taken together, these results indicate that the ASI CCN-SMPS dataset is affected by unresolved instrumental issues. As it is not possible to robustly correct these biases, we have decided to exclude the ASI site from the revised manuscript.

Consequently, the manuscript has been thoroughly revised to ensure internal consistency. Specifically, ASI has been removed from the text and analyses, and Figures 1-4, Table 1, the Dcrit-based discussion (and consequently Figure 11) have been updated. In addition, figures and tables in the Supplement have been revised: Tables S2 and S5

(now Tables S4 and S7), and Figures S1 (now Figure S5), S4c (now Figure S9c), and S14 (now Figure S19).

(7) Throughout the manuscript the activation diameters are referred to as “critical diameters”. This usage has unfortunately become more common in the literature. Usually in Köhler theory the term “critical diameter” is used for the ambient particle diameter at activation (i.e. the diameter indicating the maximum of the Köhler curve, corresponding to Scrit). I would encourage the use of another term, such as “(dry) activation diameter”, but I leave this up to the authors.

We agree that, strictly within Köhler theory, the term *critical diameter* refers to the wet particle diameter at activation corresponding to the maximum of the Köhler curve (i.e., at SScrit). In this study, however, we use *critical diameter* to denote the dry particle diameter required for activation at a given supersaturation, following the terminology adopted in in the considered database (Andrews et al., 2025b) and in the associated manuscript (Andrews et al., 2025a), as well as in Schmale et al. (2018). To avoid ambiguity, we have clarified this definition explicitly in Section 2.3 CCN-derived properties in the manuscript.

Line 164-166 (lines 167-171 in the revised manuscript)- *‘The critical diameter (Dcrit) represents the particle size above which all particles are activated into cloud droplets at a given SS. While the term critical diameter is sometimes used in Köhler theory to refer to the wet particle diameter at the maximum of the Köhler curve (corresponding to SScrit), we follow the terminology adopted in the considered data set (Andrews et al., 2025b) and associated manuscript (Andrews et al., 2025a), as well as in Schmale et al. (2018), where Dcrit denotes the dry diameter required for activation at a given SS.’*

<u>Response to referee #3 minor comments:</u>

1. Line 29: The classification of site types in this section seems confused. Urban and high-altitude sites are generally considered part of the continental region. The authors should revise this description for greater accuracy.

We thank the reviewer for this comment and agree that classifying observational sites is inherently challenging as no standardized classification exists. As noted by Laj et al. (2020), “no simple site characterization can completely capture the influences on a location”; site labels are therefore pragmatic, process-based descriptors rather than a definitive categorization. Guided by this perspective, our classifications were chosen to reflect the dominant environmental influences reported for each location in the literature (e.g., ocean proximity, boundary-layer conditions, elevation, and local emission sources). Several sites show mixed influences and are given dual classifications where appropriate

(e.g., mountain/continental, marine/polar). For transparency, brief justifications for each site classification are provided below with supporting references.

• ANX (Marine/Polar) - Coastal site near Andenes (69°N, 16°E), deployed in the COMBLE campaign to study cold-air outbreaks in the marine boundary layer (Geerts et al., 2022).

• COR (Continental) - Sierras de Córdoba (central Argentina), subtropical midlatitude continental region with few prior aerosol field campaigns (Fast et al., 2024).

• ENA (Marine) - Eastern North Atlantic, remote region with clean marine environment and persistent subtropical marine boundary-layer clouds (Wood et al., 2015; Gallo et al., 2020).

• GUC (Mountain/Continental) - High-altitude site (3137 m) in a continental interior mountain valley near Crested Butte, Colorado; orographic and continental characteristics documented by the SAIL campaign (Feldman et al., 2023).

• MAO (Continental/Urban) - Central Amazonian site occasionally influenced by urban emissions from the nearby municipality of Manacapuru (Varanda Rizzo et al, 2018).

• MOS (Marine/Polar) - Arctic site observed during the MOSAiC expedition aboard RV Polarstern (Shupe et al., 2022).

• SBS-SPL (Continental/Mountain) - Storm Peak Laboratory (3220 m), mountain-top remote site; aerosol properties consistent with previous reports for remote continental locations (Hallar et al., 2016; Friedman et al., 2013).

• SBS-CP (Continental / Mountain) - Christy Peak, adjacent to SBS-SPL (2438 m), within the same complex terrain.

• SGP (Continental) - Designed to represent a midlatitude, midcontinental environment (Sisterson et al., 2016).

On the basis of the literature cited above and the pragmatic, process-based approach advocated by Laj et al. (2020), we consider the current site labels a justified and transparent summary of the dominant influences at each location.

2. Line 144: The authors frequently refer to figures in the supplement of Andrews et al. (2025a). I suggest that the authors reproduce these validation plots using the original data and include them in the appendix of the current manuscript. Requiring readers to consult the appendix of another paper is inconvenient and may hinder understanding.

Thank you for your suggestion and for highlighting the importance of accessibility for readers. We fully understand that consulting figures from another paper can be

inconvenient. However, reproducing the validation plots from Andrews et al. (2025a) would essentially duplicate material that has already been published, significantly increasing the length of the supplementary section, and we believe this information is not essential for following the results presented in this manuscript.

We would like to emphasize that both manuscripts and database are open access and can be easily consulted if needed. However, in order to address this concern, we have ensured that the manuscript provides clear references and concise explanations so that readers can easily locate and interpret the relevant information in Andrews et al. (2025a).

3. Line 164: It is unclear how the authors determined the critical diameter—was it measured using combined CCNc and SMPS, or obtained by another method? The authors should clarify this and provide the relevant calculation formulas in the main text or the Supplement.

The procedure for determining the critical diameter is described in lines 165–166: "It can be derived by integrating the PNSD from the largest to the smallest diameters until the integrated number matches the measured CCN concentration at a given SS". However, to further clarify and improve readability, we have now included the corresponding calculation formula in line 176.

Line 165-166 (lines 171-173 in the revised manuscript)- '*It can be derived by integrating the PNSD from the largest to the smallest diameters (Eq. 1) until the integrated number matches the measured CCN concentration at a given SS (Vogelmann et al., 2012; Jurányi et al., 2011).'*

$$N_{\mathrm{CCN}}(\mathrm{SS}) = \int_{D_{\mathrm{crit}}(\mathrm{SS})}^{D_{\max}} \frac{dN}{d\log D}\, d\log D$$

4. Line 376: Here the authors use "SO42-, NO3-…", while they use "sulfate, nitrate…" in the Figure 3.

The notation has been made consistent between the text and Figure 3 by explicitly indicating the chemical species (e.g., sulfate as SO_4^{2-} and nitrate as NO_3^-) in the figure.

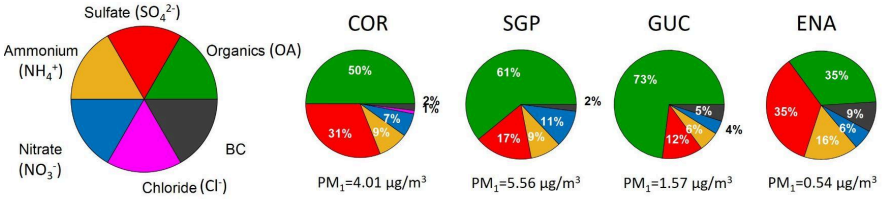

Figure R6. Pie chart of PM1 mass concentration (OA, SO_4^{2-}, NO_3^-, NH_4^+, Cl^- and BC) averaged for all the sites. Total mean PM1 mass concentration for each site included.

5. Line 379: The font of the symbols “µg/m3” here differs from that used in line 383.

The font of the symbols on line 383 (line 387 in the revised manuscript) has been corrected to match line 379, and the units are now set in italic for consistency throughout the manuscript.

6. Figure 4b: The denominator “IA+OA” is missing parentheses.

Parentheses have been added to the denominator “IA+OA” in Figure 4b, as well as in Figure S3 (Figure S8 in the new version of the manuscript) of the Supplement.

7. Figure 5: Please specify in the figure caption how the number of points in the filled areas was determined.

The number of points in the filled areas of Figure 5 was determined using a 2D histogram approach. Specifically, all paired measurements of observed vs. predicted CCN concentrations at each supersaturation were binned into 105×105 log-spaced bins along both axes. The color intensity of each filled bin in the figure corresponds to the number of points within that bin, providing a visual representation of the density of paired data. This procedure is now clearly described in the figure caption of the revised manuscript.

‘Figure 5. Log-log scatter plot of predicted CCN concentrations (N_{CCN} pred) with respect to the observed CCN concentrations (N_{CCN} meas) for all SS for all the sites using the three prediction schemes. Colored areas indicate the density of paired measurements, with color intensity representing the number of points within each log-spaced 2D bin (105×105 bins). A boxplot showing the relative bias is included- the central line represents the median, the box edges correspond to the 25th and 75th percentiles, and the whiskers extend from the ends of the interquartile range (IQR) to the most extreme data points within 1.5 times the IQR. Plots correspond to (a) Scheme 1 ($\kappa_{chem,Sch1}$), (b) Scheme 2 ($\kappa_{chem,Sch2}$) and (c) Scheme 3 (fixed κ_{chem}). The solid black line represents the 1:1 line and the dashed lines are the +/-50%.’

8. Line 496: The citation format here is incorrect; it should be “Saliba et al., 2020.” Please check for similar errors elsewhere in the manuscript.

The citations previously mentioned on line 496 are no longer included in the revised manuscript due to changes in the text. However, we have carefully checked the manuscript for similar formatting errors to ensure consistency throughout.

9. Figure 7, Figure 8c, and Figure 9c: The same question for Figure 5.

The captions of Figures 7, 8c, 9c, as well as Figures S13 (now Figure S18) and S14(a) (now Figure S19a) in the Supplement, have been treated in the same way as Figure 5 (see our response to comment 7) to indicate how the number of points in the filled areas was

calculated. Specifically, they now include a description of the 2D histogram approach, where the color intensity represents the number of valid paired points within each bin.

10. Figure 10: Please show colorbar for this heatmap.

The figure 10 has been updated to include a colorbar, which indicates the same information described in the caption: the variable with the highest importance in each prediction is shown in red; importance values ≥0.20 are shown in orange; values between 0.15 and 0.19 are shown in dark yellow; and values <0.15 are shown in light yellow.

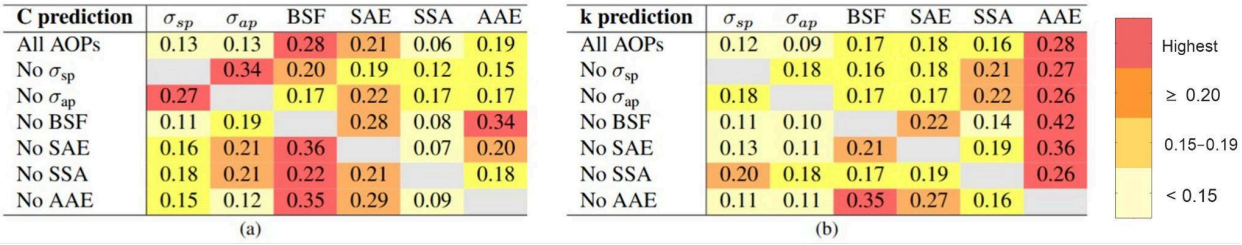

Figure R7. Heatmap of input variable importance in the Random Forest model for (a) C and (b) k parameters. Each row corresponds to a RF model in which one AOP has been removed, while each column represents the importance assigned to each available AOP in that model. The variable with the highest importance in each prediction is shown in red; importance values ≥0.20 are shown in orange; values between 0.15 and 0.19 in dark yellow; and values <0.15 in light yellow.

References

Andrews, E., Zabala, I., Carrillo-Cardenas, G., Titos, G., Casquero-Vera, J. A., and Hallar, A. G. (2025a). Harmonized aerosol size distribution, cloud condensation nuclei, chemistry and optical properties at 10 sites. *Scientific Data*, 12.

Andrews, E., Zabala, I., Carrillo-Cardenas, G., Titos, G., Casquero-Vera, J. A., and Hallar, A. G. (2025b). Harmonized aerosol size distribution, cloud condensation nuclei, chemistry and optical properties at 12 sites. Dataset, https://doi.org/10.6084/m9.figshare.27913806.v1.

Che, H., Zhang, L., Segal-Rozenhaimer, M., Dang, C., Zuidema, P., and Sedlacek, A. J. I. (2025). Aerosol hygroscopicity over the South-East Atlantic Ocean during the biomass burning season – Part 2: Influence of sea salt and burning conditions on CCN hygroscopicity, Atmospheric Chemistry and Physics, 25, 10 987–11 002.

Fast, J. D., Varble, A. C., Mei, F., Pekour, M., Tomlinson, J., Zelenyuk, A., Sedlacek III, A. J., Zawadowicz, M., and Emmons, L. K. (2024). Large Spatiotemporal Variability in Aerosol Properties over Central Argentina during the CACTI Field Campaign. *Atmospheric Chemistry and Physics*, 24.

Feldman, D. R., Aiken, A. C., Boos, W. R., *et al.* (2023). The Surface Atmosphere Integrated Field Laboratory (SAIL) Campaign. *Bulletin of the American Meteorological Society*, 104, E2192–E2222.

Friedman, B., Zelenyuk, A., Beranek, J., Kulkarni, G., Pekour, M., Hallar, A. G., McCubbin, I. B., Thornton, J. A., and Cziczo, D. J. (2013). Aerosol measurements at a high-elevation site: Composition, size, and cloud condensation nuclei activity. *Atmospheric Chemistry and Physics, 13*(23), 11839–11851.

Gallo, F., Uin, J., Springston, S., Wang, J., Zheng, G., Kuang, C., Wood, R., Azevedo, E. B., McComiskey, A., Mei, F., Theisen, A., Kyrouac, J., and Aiken, A. C. (2020). Identifying a regional aerosol baseline in the eastern North Atlantic using collocated measurements and a mathematical algorithm to mask high-submicron-number-concentration aerosol events. *Atmospheric Chemistry and Physics*, 20, 7553–7573.

Geerts, B., Giangrande, S. E., McFarquhar, G. M., *et al.* (2022). The COMBLE Campaign: A Study of Marine Boundary Layer Clouds in Arctic Cold-Air Outbreaks. *Bulletin of the American Meteorological Society*, 103, E1371–E1389.

Hallar, A. G., Petersen, R., McCubbin, I. B., Lowenthal, D., Lee, S., Andrews, E., and Yu, F. (2016). Climatology of new particle formation and corresponding precursors at Storm Peak Laboratory. *Aerosol and Air Quality Research, 16*, 816–826.

Hastie, T., Tibshirani, R., and Friedman, J. (2009). *The Elements of Statistical Learning: Data Mining, Inference, and Prediction* (2nd ed.). Springer.

Howes, C., Saide, P. E., Coe, H., Dobracki, A., Freitag, S., Haywood, J. M. *et al*. (2023). *Biomass-burning smoke's properties and its interactions with marine stratocumulus clouds in WRF-CAM5 and southeastern Atlantic field campaigns,* Atmospheric Chemistry and Physics, 23, 21 13911–13940.

Laj, P., Bigi, A., Rose, C., Andrews, E., Myhre, C. L., *et al.* (2020). A global analysis of climate-relevant aerosol properties retrieved from the network of Global Atmosphere Watch (GAW) near-surface observatories. *Atmospheric Measurement Techniques*, 13, 4353–4392.

Rizzo, L. V., Roldin, P., Brito, J., Backman, J., Swietlicki, E., Krejci, R., Tunved, P., Petäjä, T., Kulmala, M., and Artaxo, P. (2018). Multi-year statistical and modeling analysis of submicrometer aerosol number size distributions at a rain forest site in Amazonia. *Atmospheric Chemistry and Physics, 18*(14), 10255–10274.

Shupe, M. D., Rex, M., Blomquist, B., *et al.* (2022). Overview of the MOSAiC expedition. Atmosphere, *Elementa: Science of the Anthropocene*, 10, 00060.

Sisterson, D. L., Peppler, R. A., Cress, T. S., Lamb, P. J., and Turner, D. D. (2016). The ARM Southern Great Plains (SGP) Site. *American Meteorological Society Monographs, 6*, 6.1–6.14.

Wood, R., Wyant, M., Bretherton, C. S., *et al.* (2015). Clouds, Aerosols, and Precipitation in the Marine Boundary Layer: An ARM Mobile Facility Deployment. *Bulletin of the American Meteorological Society*, 96, 419–440.